Work supported by the Swiss State Secretariat for Education, Research and Innovation SERI

Electron cloud

L. Mether

I. Bellafont, G. Rumolo

FCC Week 2018, Amsterdam
April 9th-13th 2018

Introduction

Electron clouds can cause transverse instabilities, tune shift and spread, emittance growth, losses, heat load and vacuum degradation

- Effects can effectively be mitigated by preventing the build-up of electron clouds
- Need to identify required conditions to sufficiently suppress electron cloud build-up

Previous studies

E-cloud studies for 25 ns, 12.5 ns and 5 ns beams:

- Build-up in arc dipoles, quadrupoles, drifts
- Effect of photoelectrons
- Beam dynamics simulations to confirm instability thresholds

Studies performed using

- Main chamber of beam screen (2015 version)
- Cu surface

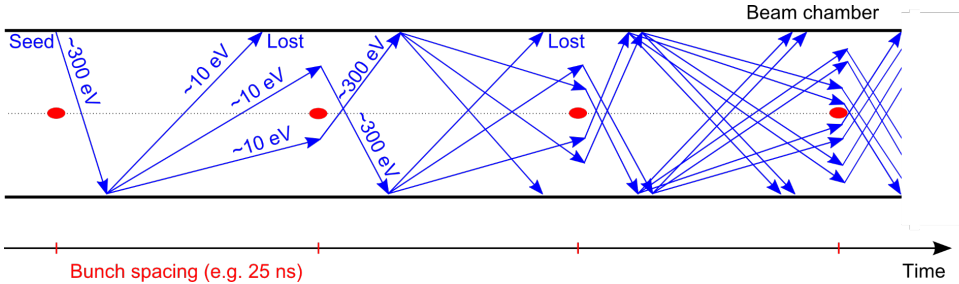

New results

- Cloud distribution and beam screen geometry
- Bunch train pattern and other updated parameters
- Photoelectrons according to distribution from ray tracing

Overview of previous results

Results of build-up studies (no photoelectrons):

- Multipacting thresholds for the 25 ns beam are moderate, and build-up can be efficiently suppressed with coatings
- Tighter constraints for alternative bunch spacings, especially 12.5 ns → maximum SEY no larger than 1 may be needed for full suppression

Multipacting thresholds for build-up
(Highest SEY without build-up)

	25 ns		12.5 ns		5 ns	
E [TeV]	3.3	50	3.3	50	3.3	50
Dipole	1.6	1.6	1.2	1.2	1.5	1.4
Quad	1.2	1.3	1.0	1.1	1.1	1.1
Drift	1.8	1.8	1.2	1.2	1.5	1.4

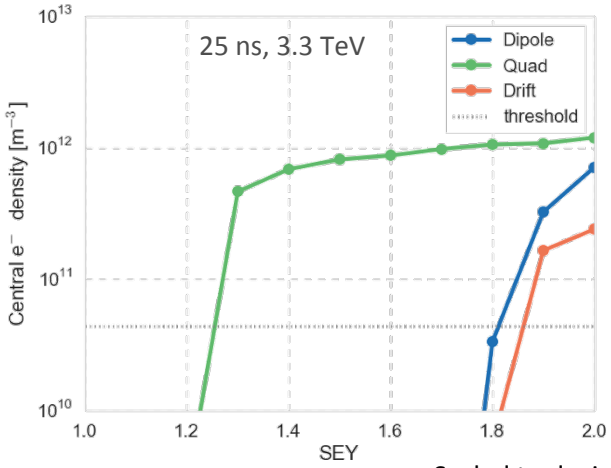

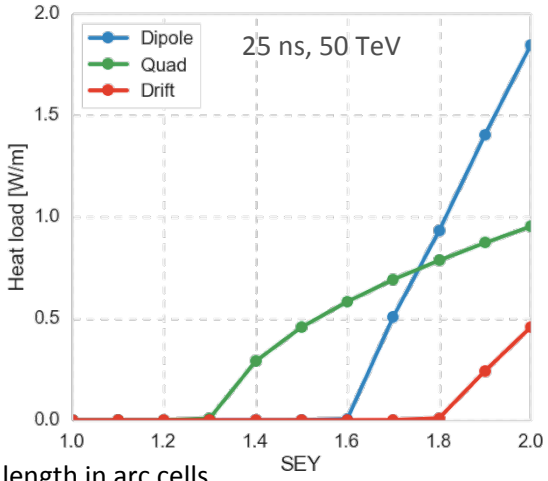

Scaled to device length in arc cells

Main conclusions:

- Heat loads with 25 ns are moderate compared to the synchrotron radiation ~28.4 W/m
- Stability is critical: central densities are above the instability threshold in most cases if build-up occurs, in particular in the quadrupoles and for the smaller bunch spacings

Cloud distribution

The cloud distributions have been identified in order to determine where beam screen coating is required

Dipole

The coating should cover the full top and bottom of the chamber

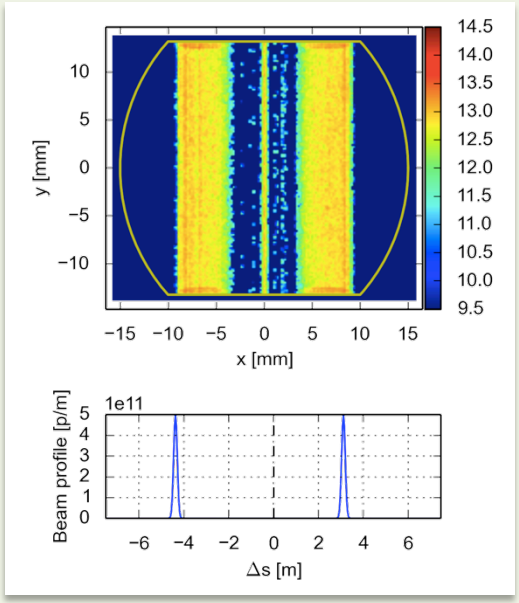

Quadrupole

Coating is required at 45° to the horizontal plane

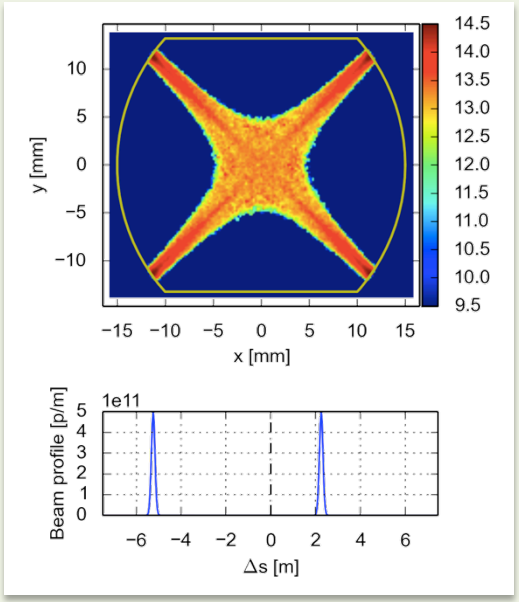

Drift

Multipacting on all sides, hot spots along horizontal and vertical axes

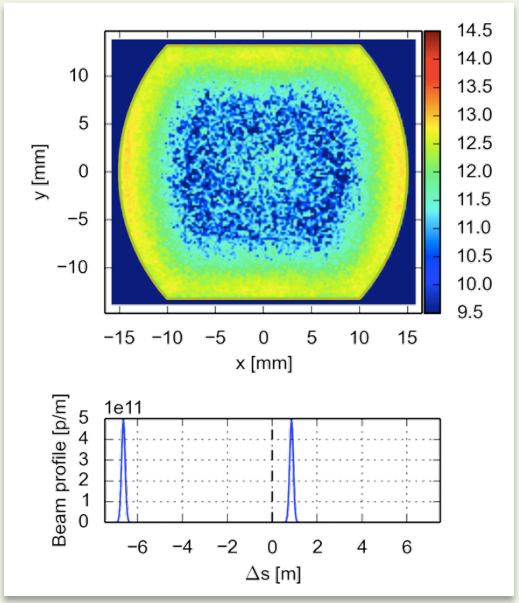

Effect of beam screen design

Evolution of beam screen design:

2015 → 2017
- Larger slit, saw-tooth surface, straight edges
- Impact expected mainly in the drifts, due to the cloud distribution in magnetic fields

2017 → 2018
- Smaller vertical aperture (by 2 mm)
- Could impact results also in dipoles and quads

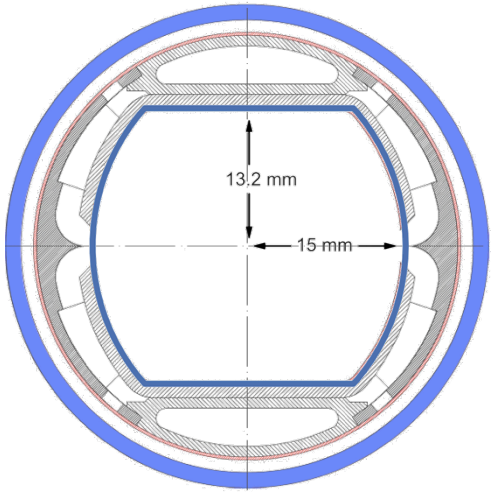

2015

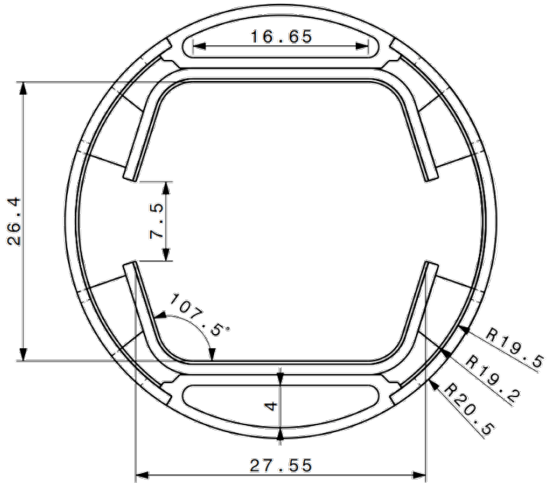

2017

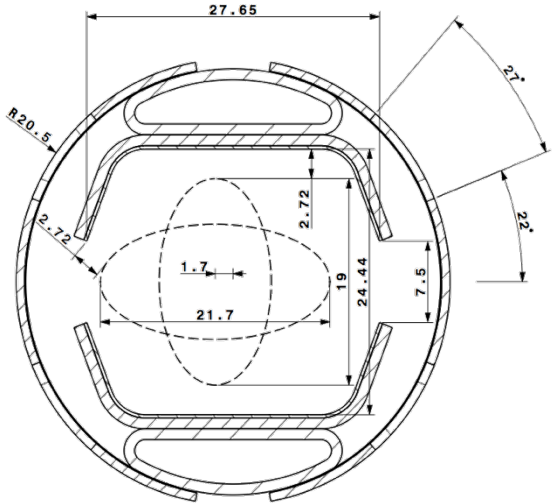

2018

C. Garion, J. Fernandez Topham et al, *see talk of F. Perez*

Effect of beam screen design

2015 → 2017

The threshold in the drift is pushed higher,
no other significant effect

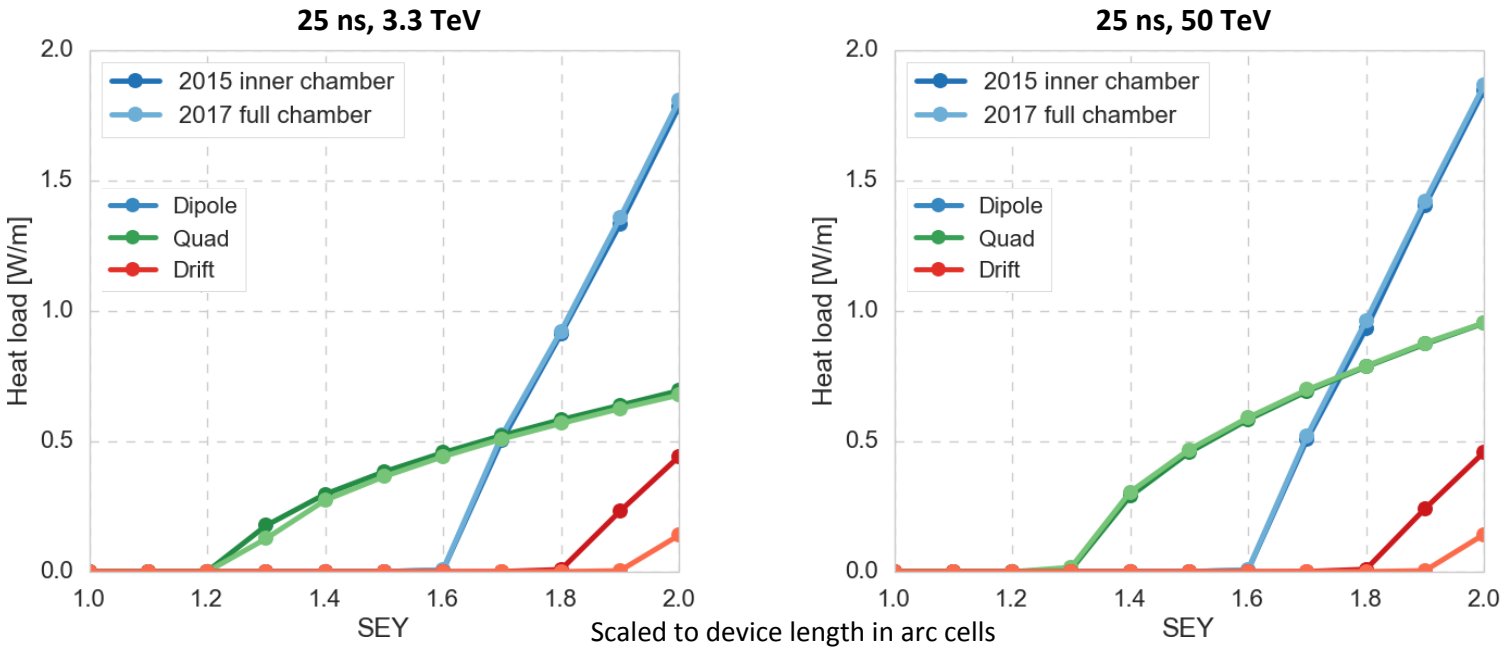

Scaled to device length in arc cells

Effect of beam screen design

2015 → 2017

The threshold in the drift is pushed higher, no other significant effect

2017 → 2018

The drift threshold is increased further, and the dipole threshold is slightly increased as well

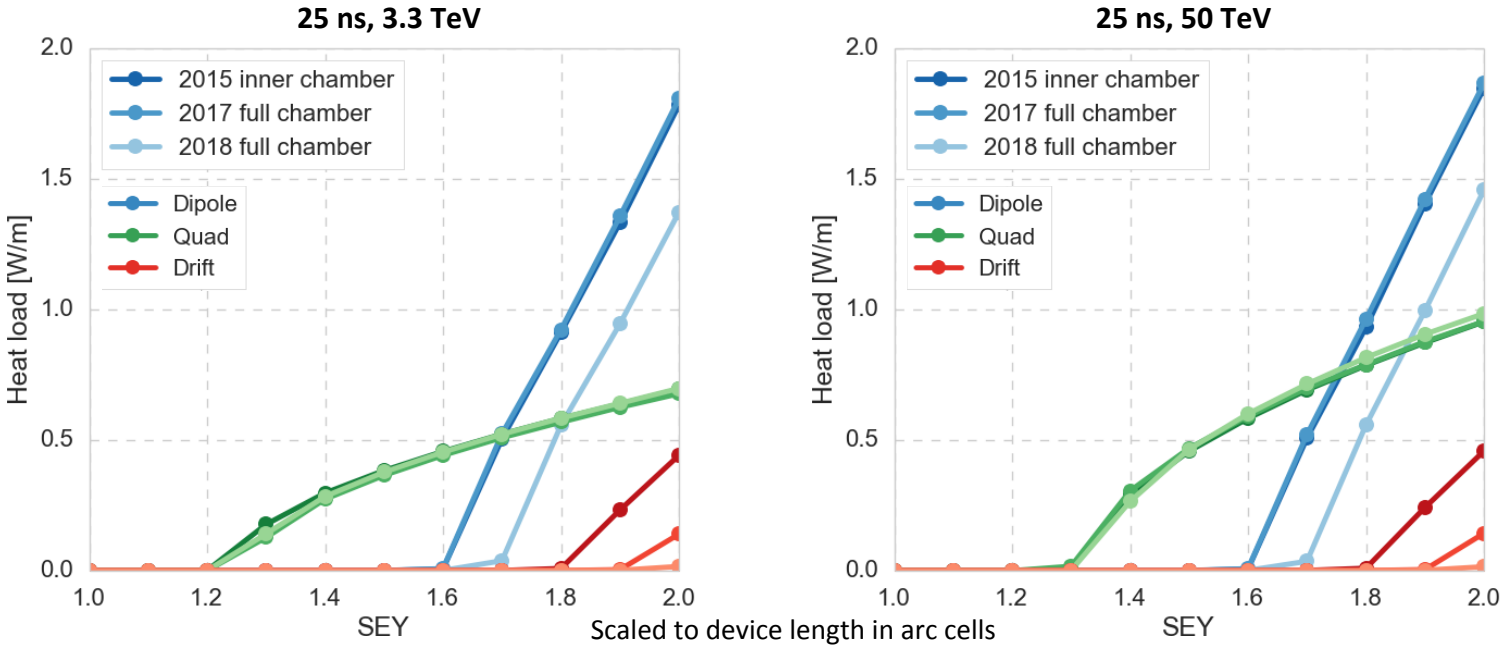

Effect of beam screen design

2015 → 2017
The threshold in the drift is pushed higher, no other significant effect

2017 → 2018
The drift threshold is increased further, and the dipole threshold is slightly increased as well

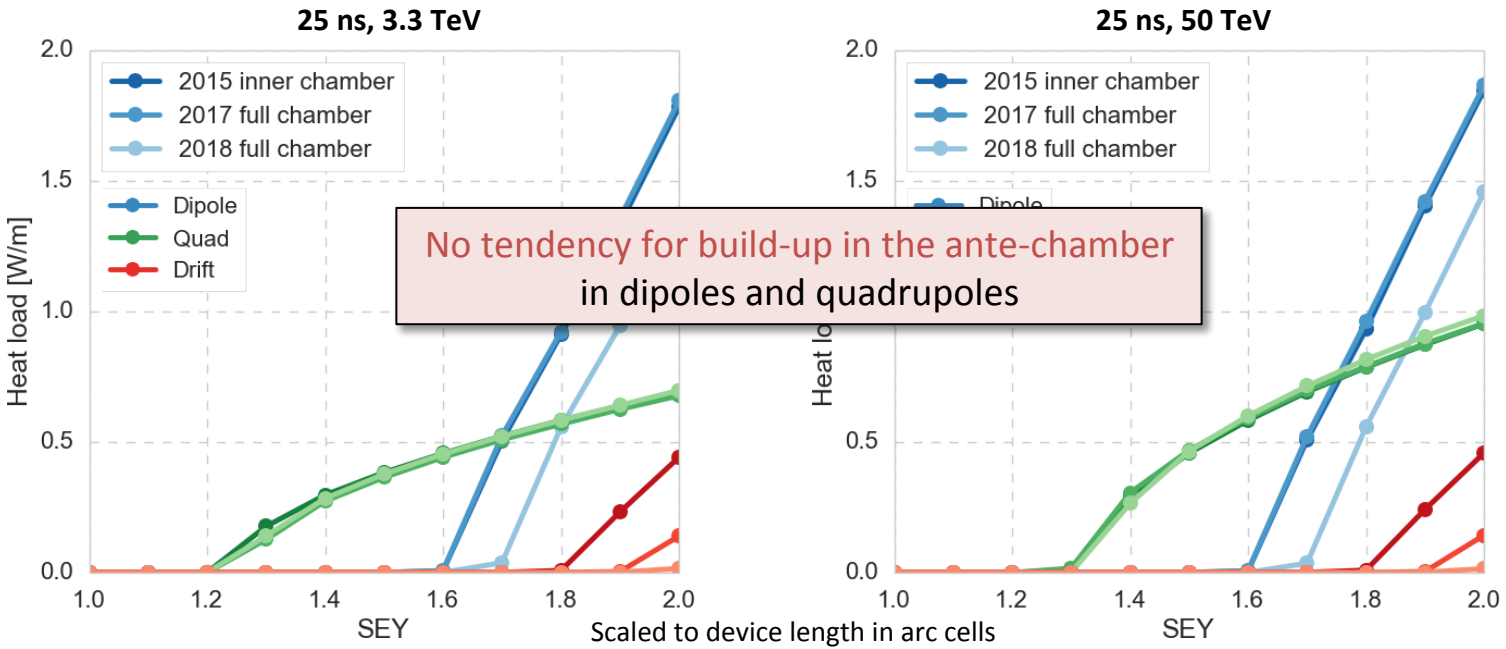

Updated parameters

- Bunch train pattern defined by injection considerations
  Previously used 50 bunches + 12 empty slots for the 25 ns beam → 80 bunches + 17 empty slots
- Arc element lengths
- Magnet strengths

Simulation parameters in 2018			
Bunch spacing [ns]	25	12.5	5
Bunch intensity [p^+]	10×10^{10}	5×10^{10}	2×10^{10}
Norm. emittance [m]	2.2e-6	1.1e-6	0.44e-6
Bunch length [m]	0.08		
Bunch train pattern	80b + 17e	160b + 34e	400b + 85e
Arc elements	**Dipole:** 16 T, 78.4 % of arc length		
	Quadrupole: 380 T/m, 6.4 % of arc length 9.7 % of arc length with multipoles		
	Drift: 10.7 % of arc length		

Updated parameters

- Bunch train pattern defined by injection considerations
  Previously used 50 bunches + 12 empty slots for the 25 ns beam → 80 bunches + 17 empty slots
- Arc element lengths
- Magnet strengths

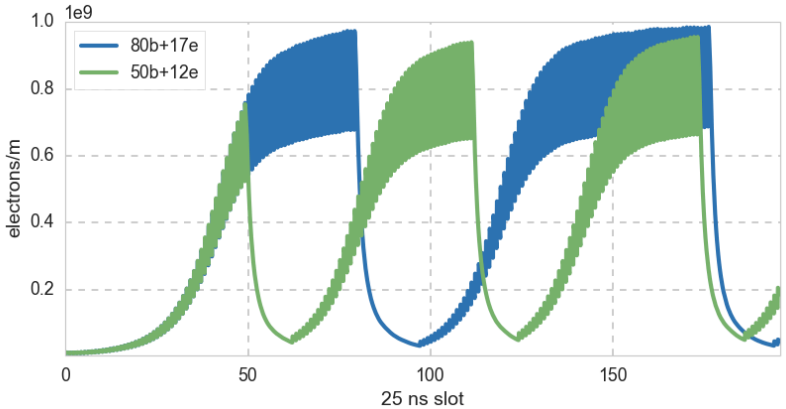

The increase in train length has a stronger effect than the increase in gap length
→ generally lower multipacting thresholds

Simulation parameters in 2018			
Bunch spacing [ns]	25	12.5	5
Bunch intensity [p^+]	10 x 10^{10}	5 x 10^{10}	2 x 10^{10}
Norm. emittance [m]	2.2e-6	1.1e-6	0.44e-6
Bunch length [m]	0.08		
Bunch train pattern	80b + 17e	160b + 34e	400b + 85e
Arc elements	**Dipole:** 16 T, 78.4 % of arc length		
	Quadrupole: 380 T/m, 6.4 % of arc length 9.7 % of arc length with multipoles		
	Drift: 10.7 % of arc length		

Updated parameters

- Lower multipacting thresholds in the dipoles and quadrupoles
- For the alternative bunch spacings the lower thresholds are particularly constraining:

Central densities are above the instability threshold even for low SEY above the threshold → full suppression needed for beam stability

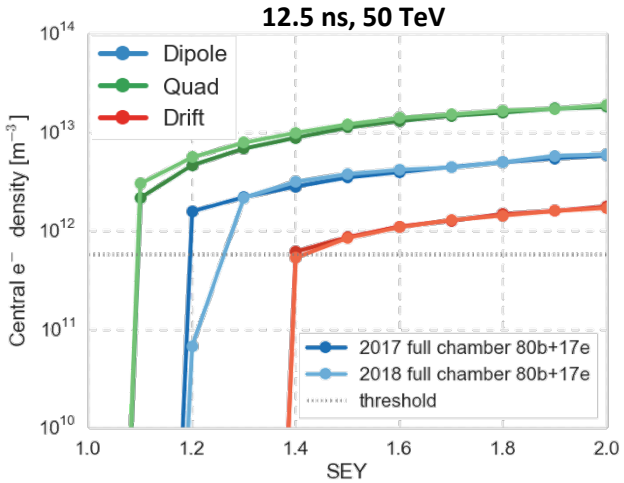

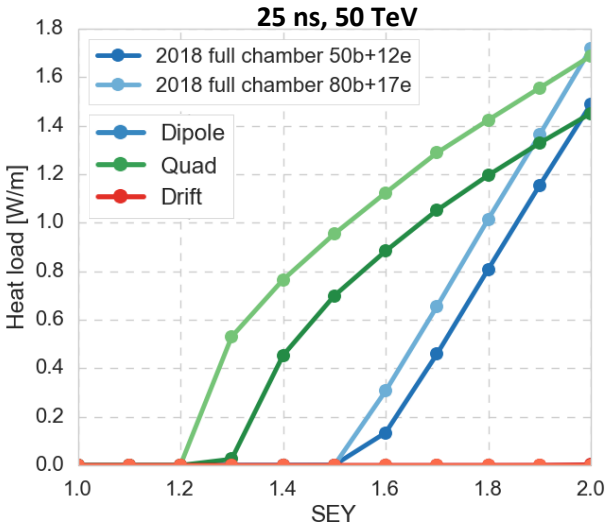

Multipacting thresholds with 2017 / 2018 chamber
(highest max SEY without build-up)

	25 ns		12.5 ns		5 ns	
E [TeV]	3.3	50	3.3	50	3.3	50
Dipole	1.4 / 1.5	1.4 / 1.5	1.1	1.1	1.5	1.5
Quad	1.2 / 1.1	1.2	1.0	1.0	1.1	1.0
Drift	2.0	2.0	1.3	1.3	1.6	1.6

Photoelectrons

Previous studies showed that photoelectrons could raise the central density above the instability threshold also below the multipacting threshold, especially for the 12.5 and 5 ns beams

- Constraints on the photoelectron flux were estimated and considered by the beam screen design team, which found the 2017 model with saw-tooth compatible in dipoles and quadrupoles

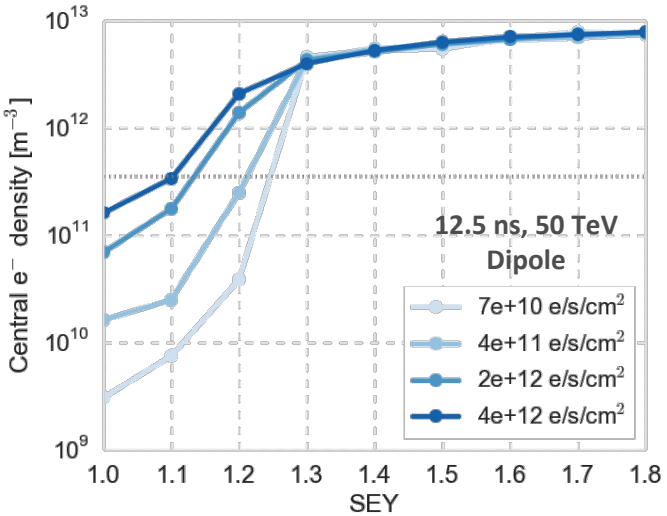

I. Bellafont

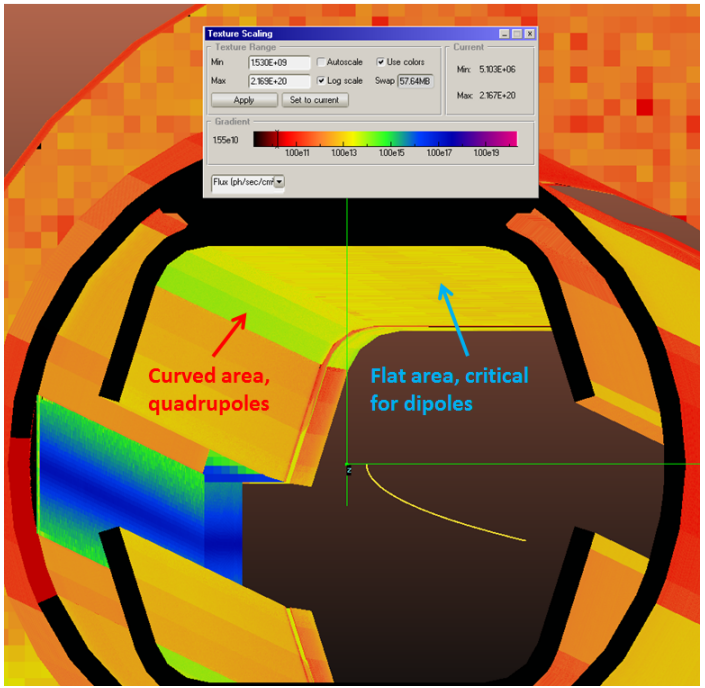

Photoelectrons

Previous studies showed that photoelectrons could raise the central density above the instability threshold also below the multipacting threshold, especially for the 12.5 and 5 ns beams

- Constraints on the photoelectron flux were estimated and considered by the beam screen design team, which found the 2017 model with saw-tooth compatible in dipoles and quadrupoles

I. Bellafont

Photoelectron flux distributions based on ray-tracing studies implemented in the build-up simulations:

- Conservative estimate (10% photoyield, 0% reflection): photoelectron flux 5×10^{10} – 5×10^{11} e/cm^2/s on inner surfaces
- LASE estimate: photoelectron flux 10^9 – 10^{10} e/cm^2/s on inner surfaces

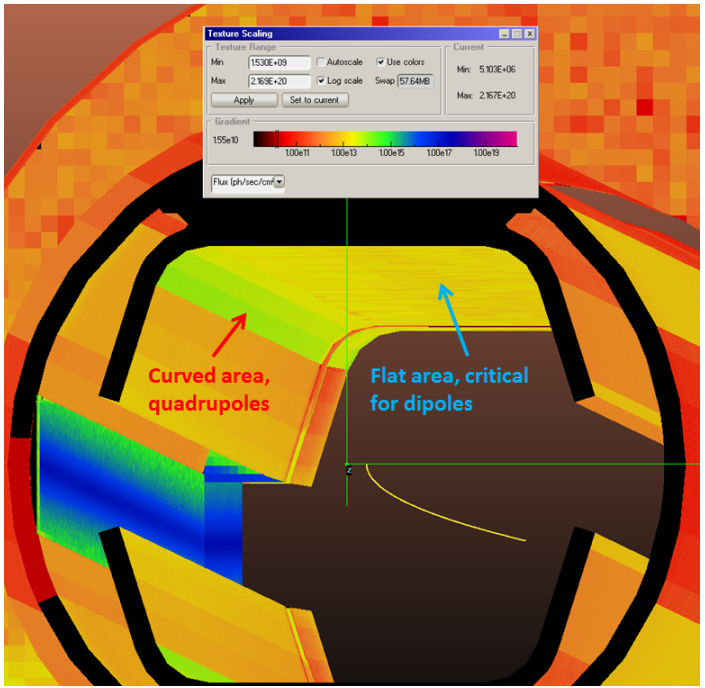

Photoelectrons

Previous studies showed that photoelectrons could raise the central density above the instability threshold also below the multipacting threshold, especially for the 12.5 and 5 ns beams

- Constraints on the photoelectron flux were estimated and considered by the beam screen design team, which found the 2017 model with saw-tooth compatible in dipoles and quadrupoles

Photoelectron flux distributions based on ray-tracing studies implemented in the build-up simulations:

- Conservative estimate (10% photoyield, 0% reflection): photoelectron flux 5×10^{10} – 5×10^{11} e/cm^2/s on inner surfaces
- LASE estimate : photoelectron flux 10^9 – 10^{10} e/cm^2/s on inner surfaces

Simulations confirm that both cases are viable

- Central electron densities remain below the instability threshold for all bunch spacings when the SEY is below the multipacting threshold

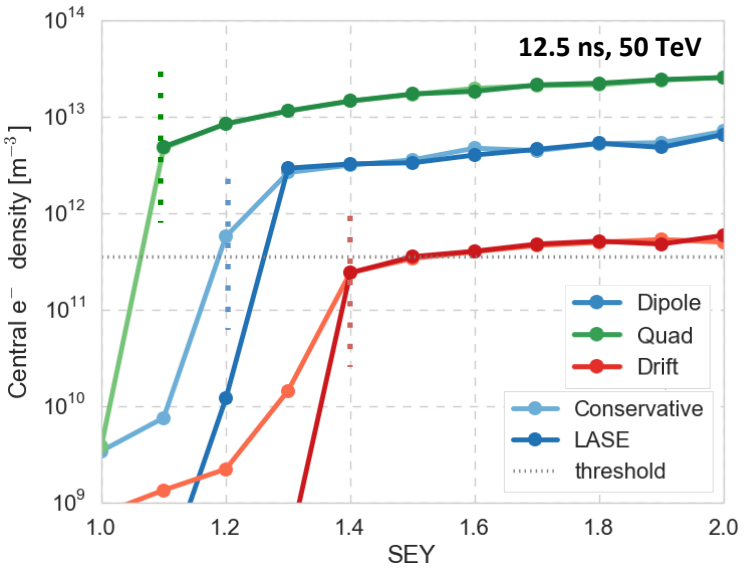

Photoelectrons

Previous studies showed that photoelectrons could raise the central density above the instability threshold also below the multipacting threshold, especially for the 12.5 and 5 ns beams

- Constraints on the photoelectron flux were estimated and considered by the beam screen design team, which found the 2017 model with saw-tooth compatible in dipoles and quadrupoles

I. Bellafont

Photoelectron flux distributions based on ray-tracing studies implemented in the build-up simulations:

- Scanned flux on saw-tooth area in range 10^{12} – 10^{13} e/cm^2/s

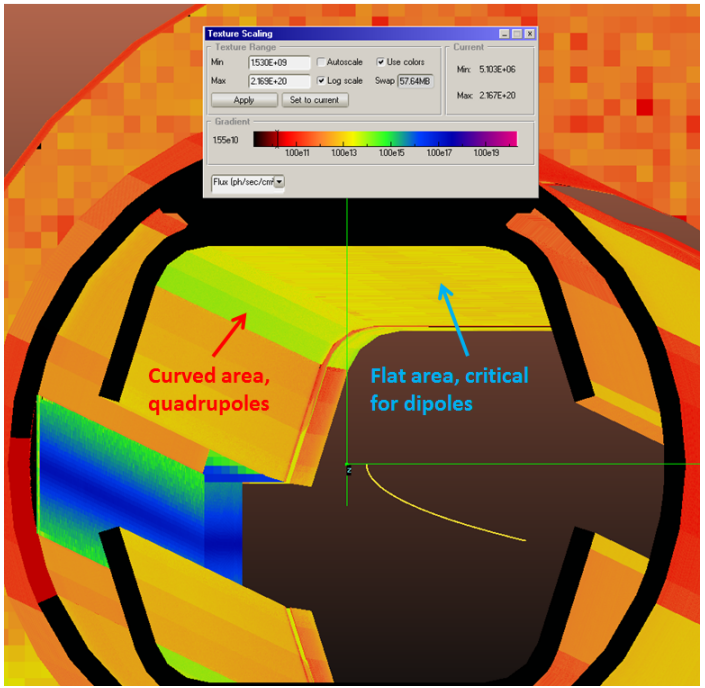

Photoelectrons

Previous studies showed that photoelectrons could raise the central density above the instability threshold also below the multipacting threshold, especially for the 12.5 and 5 ns beams

- Constraints on the photoelectron flux were estimated and considered by the beam screen design team, which found the 2017 model with saw-tooth compatible in dipoles and quadrupoles

Photoelectron flux distributions based on ray-tracing studies implemented in the build-up simulations:

- Scanned flux on saw-tooth area in range 10^{12} – 10^{13} e/cm^2/s

The flux in the saw-tooth area affects the build-up mainly in field-free regions

- For the considered fluxes, central densities remain below the instability threshold for all bunch spacings when the SEY is below the multipacting threshold

Maximum expected flux in the saw-tooth area to be confirmed with beam screen design team

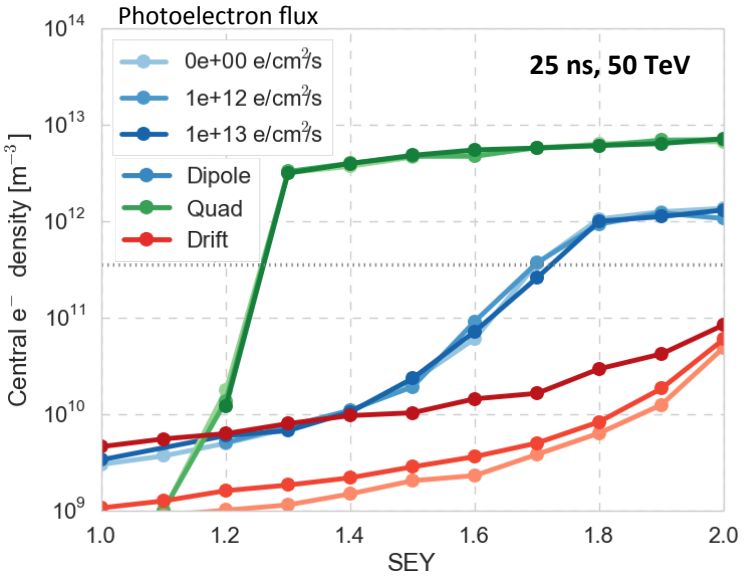

Conclusion

The effect of beam screen geometry on e-cloud build-up evaluated

- The large slit increases multipacting threshold in drifts
- No significant difference between 2017 and 2018 geometries

Conditions to suppress build-up defined with full chamber and updated parameters

- An amorphous carbon coating or LASE surface should be sufficient to suppress build-up for the 25 ns beam
  - Coating required in dipoles and quadrupoles, should not be necessary in drifts unless significant photoelectron production occurs at the saw-tooth surface
- For the alternative beams, the situation is somewhat tighter than before
  - Full suppression needed for stability → SEY ~1 in quadrupoles
  - Coating may be necessary also in field free regions

Photoelectrons initialized according to ray-tracing simulations

- Estimated photoelectron fluxes are within stability limits
- Photoelectrons from saw-tooth increases density in drifts → expected flux to be confirmed with WP4

Spares

Single bunch instability

Analytical estimate of **threshold electron density** for instability

$$\rho_{e,th} = \frac{2\gamma\nu_s\omega_e\sigma_z/c}{\sqrt{3}KQr_0\beta L} \quad \text{with} \quad \omega_e = \sqrt{\frac{\lambda_p r_e c^2}{\sigma_y(\sigma_x+\sigma_y)}}, \quad K = \omega_e\sigma_z/c, \quad Q = \min(\omega_e\sigma_z/c, 7)$$

With updated machine parameters

3.3 TeV	50 TeV
6 x 10^{10} m^{-3}	3.6 x 10^{11} m^{-3}

Above the multipacting threshold, central electron densities are in the instability regime

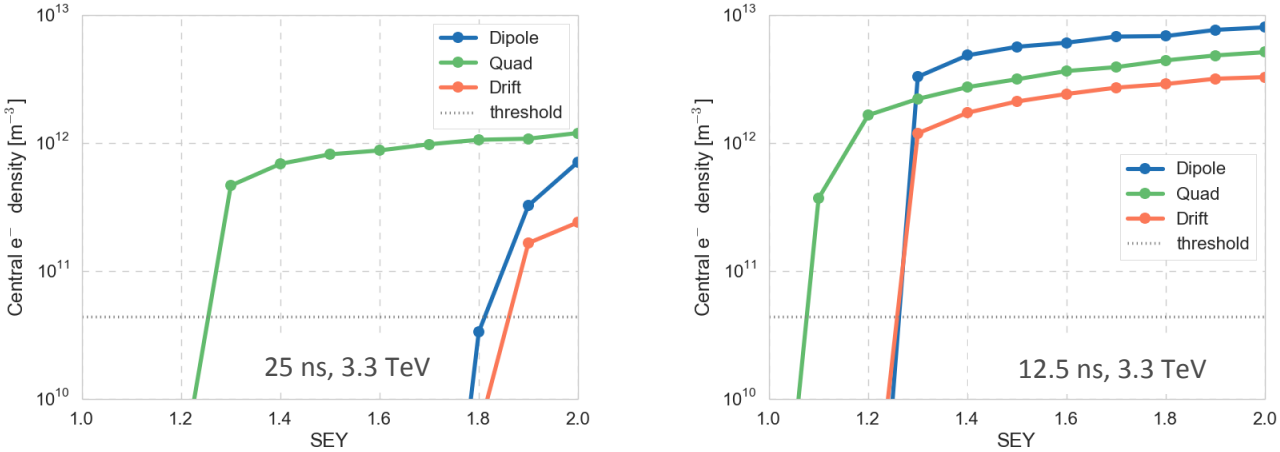

Central electron densities scaled to device length in half-cell

Single bunch instability simulations

First instability simulation study: 25 ns beam at 3.3 TeV in dipole field – no stabilizing mechanisms

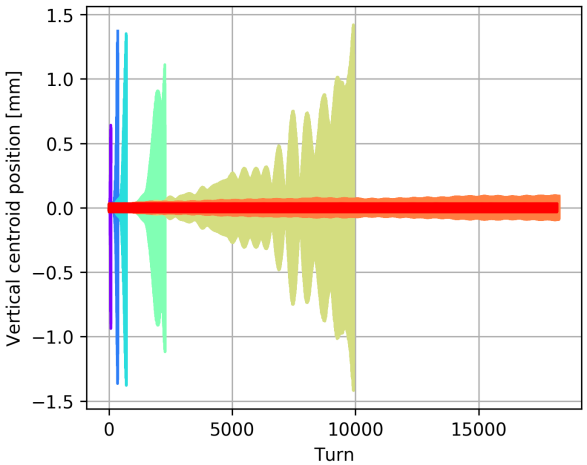

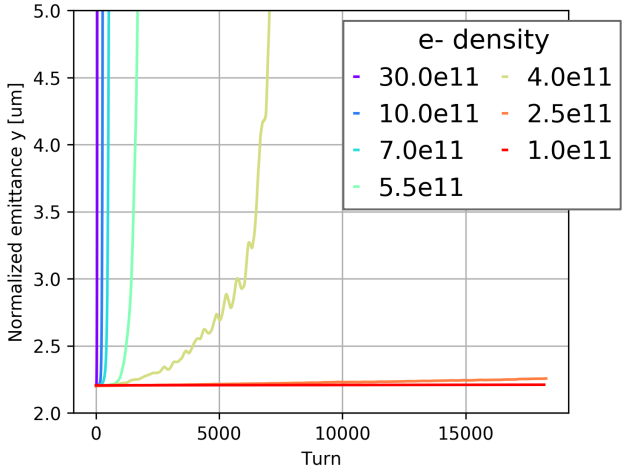

Ongoing studies:
- 5 ns at 3.3 TeV
- 25 ns at 50 TeV

→ seem to suggest similar scaling w.r.t. analytic estimate (TBC)

Over 17 000 turns (~ 5 s): instability threshold around 1-2.5 x 10^{11} m^{-3}
- Compare to analytic estimate scaled to dipole length: 7.5 x 10^{10} m^{-3}

→ Analytic estimate slightly pessimistic, by factor 2-3

Stability at injection

Electron densities at 3.3 TeV much below instability threshold

- Due to smaller number of photons, and critical energy below Cu work function

	FCC	FCC Injection		
E [TeV]	50	1.5	3.3	5.5
E_c [eV]	4030	0.11	1.14	5.26
N_γ/p^+m	0.0497	0.00149	0.00328	0.00546
N_{eff}/N_{tot}	0.878	6.1e-20	2.5e-3	0.108
N_{eff}/p^+m	0.0436	9.1e-23	8.2e-6	5.9e-3

Most critical case for stability may be at some intermediate energy

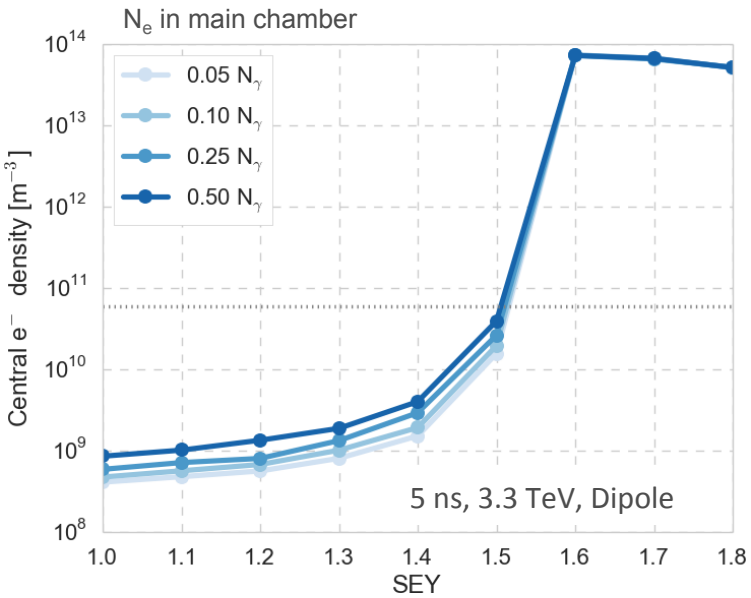

SEY model

SEY model based on extensive studies using laboratory measurements on the copper surface of the LHC beam chambers

$$\delta(E) = \delta_{\text{elas}}(E) + \delta_{\text{true}}(E)$$

$$\delta_{\text{elas}}(E) = R_0 \left(\frac{\sqrt{E} - \sqrt{E + E_0}}{\sqrt{E} + \sqrt{E + E_0}} \right)^2 \qquad R_0 = 0.7 \quad E_0 = 150\ \text{eV}$$

$$\delta_{\text{true}}(E) = \delta_{\max} \frac{s \frac{E}{E_{\max}}}{s - 1 + \left(\frac{E}{E_{\max}} \right)^s} \qquad E_{\max} = 332\ \text{eV} \quad s = 1.35$$

$$E_{\max}(\theta) = E_{\max}(\theta = 0)\,(1 - 0.7\,(1 - \cos\theta))$$

$$\delta_{\max}(\theta) = \delta_{\max}(\theta = 0)\, e^{\frac{(1 - \cos\theta)}{2}}$$

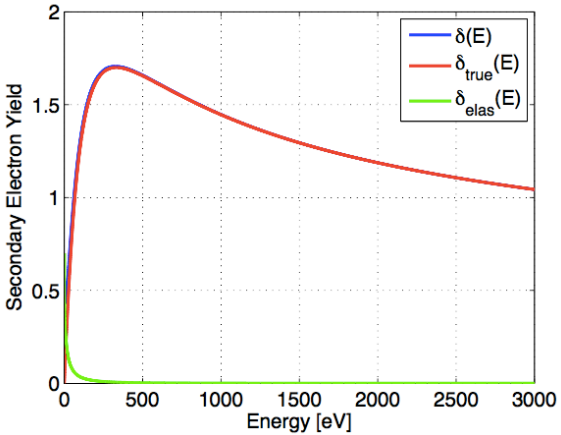

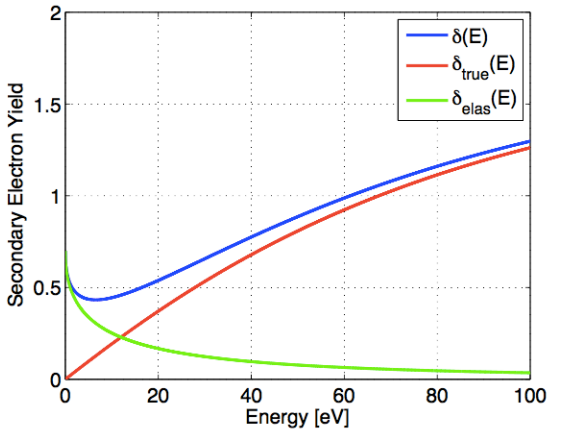

New measurements ongoing, with detailed data also at low energies

- Comparison of simulation results with standard LHC model and measured curves
- V. Petit: https://indico.cern.ch/event/685341/
  L.Bitsikokos: https://indico.cern.ch/event/714948/